Analytical Biochemistry 651 (2022) 114737

Contents lists available at ScienceDirect

Analytical Biochemistry

journal homepage: www.elsevier.com/locate/yabio

The development of a colorimetric biosensing assay for the detection of *Helicobacter pylori* in feces

Yu Fei [a,1], Rong Fang [a,1], Lina Xiao [a,b,1], Yuqing Zhang [a], Ke Fan [a], Yundi Jiang [a], Silu Lei [a], Rui Xu [c], Dailan Yang [a,b], Yan Ye [a,b], Shibing Xiang [a,b], Ping Wang [a,b], Chen Zhou [a,*], Tian Tang [a,b,**]

[a] West China School of Public Health and West China Fourth Hospital, Sichuan University, Chengdu, 610041, Sichuan, PR China
[b] West China-PUMC C.C. Chen Institute of Health, Sichuan University, Chengdu, 610041, Sichuan, PR China
[c] West China School of Stomatology, Sichuan University, Chengdu, 610041, Sichuan, PR China

ARTICLE INFO

Keywords:
Helicobacter pylori
Aptamer
Colorimetric sensing method
AuNPs
Biosensor

ABSTRACT

As *Helicobacter pylori (H. pylori)* is closely related to the occurrence of gastric diseases such as chronic gastritis, peptic ulcer, and gastric cancer, early detection of *H. pylori* is an urgent need. In this study, oligonucleotide probes conjugated with gold nanoparticles (AuNPs) were used in combination with *H. pylori*-specific aptamers for the rapid detection of *H. pylori* in stool samples, which converted the method of detection from proteins to nucleic acids. Therefore, qualitative detection of *H. pylori* can be achieved by observing color changes through the aggregation (red to purple) or deaggregation (purple to red) of AuNPs, and further quantitative detection can be achieved through UV spectrometry. The detection limit of the colorimetric biosensing method is 25 CFU/mL (S/N = 3), which is favorably comparable to other reported detection methods. Compared with the existing detection methods for *H. pylori*, this colorimetric biosensing method has no limitations to the test subjects. All these features render the colorimetric biosensing assay a promising method for the clinical field detection of *H. pylori*.

1. Introduction

Helicobacter pylori (H. pylori), a gram-negative pathogen, is related to the occurrence of many digestive disorders, such as chronic gastritis, peptic ulcer, and gastric cancer. In 1994, the World Health Organization (WHO) classified *H. pylori* as a Group 1 carcinogen [1]. The global infection rate of *H. pylori* is approximately 41% [2], while the infection rate in the Chinese population is approximately 59% [3].

At present, both invasive and noninvasive methods are employed to detect *H. pylori* [4]. Noninvasive detection (NID) methods, such as stool antigen test (SAT), antibody-based test (ABT), and C13-Urea Breath Test (C13-UBT), are more popular due to the advantages of being cost-effective, highly accurate, and user-friendly [5]. However, SAT only applied to subjects who did not take antibiotics, proton pump inhibitors (PPIs), or *N*-acetylcysteine or who suffered upper gastrointestinal bleeding. In addition, the storage temperature of samples, the time intervals before sampling and testing, and the cutoff valve also affect the outcome of SAT [4,6–8]. The ABT method cannot distinguish an active infection of *H. pylori* from post-infection [9], while the 13C-UBT method is also vulnerable to many factors, such as diet and the use of medications [10–12]. Therefore, developing a novel NID method which allows the detection of *H. pylori* in any subjects under different circumstances is an urgent need.

With the advantages of high selectivity, affinity and stability, aptamers have gained much attention for biomedical applications [13]. Previous studies have also reported that aptamers and gold nanoparticles (AuNPs) are widely used in the field of biosensing [14–17]. Given that the results of the AuNP-based colorimetric biosensing (AuNP-CB) method, which takes advantage of low cost, simplicity, and high sensitivity/specificity [18], can be easily determined by the color

* Corresponding author. 16#, Section 3, South Renmin Road, PR China.
** Corresponding author. 16#, Section 3, South Renmin Road, West China School of Public Health and West China Fourth Hospital, West China-PUMC C.C. Chen Institute of Health, Sichuan University, Chengdu, 610041, Sichuan, PR China.
E-mail addresses: zhouchen@scu.edu.cn (C. Zhou), tangtian12345@aliyun.com (T. Tang).
[1] Yu Fei, Rong Fang, and Lina Xiao contributed equally to this work and are listed as first authors.

https://doi.org/10.1016/j.ab.2022.114737
Received 23 February 2022; Received in revised form 8 May 2022; Accepted 13 May 2022
Available online 18 May 2022

change (AuNP aggregation, red-to-purple; AuNP deaggregation, purple-to-red) [19], it is not surprising that AuNP-CB methods have been widely used in clinical diagnostics, drug discovery, and environmental contaminant analysis [20].

However, there has been no research to apply AuNP-based probes and aptamers to the detection of *H. pylori.* In the present study, we developed a novel AuNP-CB method with the aim of quickly and reliably detecting *H. pylori* in stool samples. The results of the AuNP-CB method can be visually determined by the naked eye or by UV spectrometry, beneficially contributing to the timely diagnosis and treatment of *H. pylori* infection.

2. Results and discussion

2.1. Detection principle of the colorimetric biosensing method

Not recently, many colorimetric biosensing assays were developed. Their working principles, however, are different. For example, the indicator-based colorimetric biosensing assays rely on the color change of an indicator under a certain condition to determine the outcome of a test [21–24]. While the detection principle of the present method is based on the deaggregation of AuNPs. As shown in Fig. 1A, two oligonucleotide probes (probe-1 and probe-2) complemented with an *H. pylori*-specific aptamer were designed and conjugated with AuNPs (probe-1 at the 3′ end and probe-2 at the 5’ end). In the absence of *H. pylori*, the two probes bind the aptamer simultaneously. As a consequence, AuNPs aggregated due to the “end-to-end” interaction, accompanied by a color change from dark red to purple. In the presence of *H. pylori,* the binding of aptamers to the bacteria resulted in the detachment of probes, and the color of the reaction solution changed from purple to dark red. Based on this strategy, an *H. pylori*-specific colorimetric biosensing method was developed. It is important to note that the presence of oligonucleotide probes did not impact the binding of aptamer to *H. pylori*. Because both probes were detached from the aptamer in the presence of target bacteria (Fig. 1B).

2.2. Characterization of AuNPs

The AuNPs were characterized by UV–Vis spectrophotometry and transmission electron microscopy (TEM). As shown in Fig. 2A, the AuNPs presented a characteristic absorption peak at ~530 nm, while no other absorption peaks were observed, indicating that the AuNPs had a uniform size. TEM showed that the AuNPs were well separated and ellipsoid in shape with an average size of 20 nm (Fig. 2B).

2.3. Optimization of probes

As AuNPs aggregated, their color changed, and the conjugation positions of AuNPs were investigated. In one trial, we conjugated the AuNPs to the distal ends (D-AuNPs) of the two probes in a probe pair (probe-1 at the 5′ end, probe-2 at the 3′ end) and evaluated their reaction to the aptamer. The results showed that both probes successfully bound the aptamer; however, no color change was observed. A possible explanation is that the binding of D-AuNP probes to the aptamer only diminished the distance of AuNPs without causing effective aggregation. As an alternative, AuNPs were conjugated to the proximal ends of the two probes in a probe pair (probe-1 at the 3′ end, probe-2 at the 5’ end). The resulting data suggested that the color changed from dark red to purple in the presence of aptamer (data not shown), indicating that the AuNPs were successfully aggregated.

Upon acquiring the conjugation position of AuNPs, we sought to determine the optimal length of the probes. We assessed 5 pairs of probes as indicated in Table 1. The data showed that the color changed dramatically when using the probe pairs of probes-1_{20} and probes-2_{20} (Fig. 3). Therefore, the optimal length for probe-1 and probe-2 was 20 bp.

2.4. The sensitivity and linear range of the colorimetric biosensing method

Serial dilutions of *H. pylori* were used to determine the sensitivity and linear range of the colorimetric biosensing method. As shown in Fig. 4A, with increasing concentrations of *H. pylori*, AuNPs were deaggregated, as indicated by a shift of the absorption peak to a lower wavelength. In addition, the colors of the AuNP solution changed from purple to dark

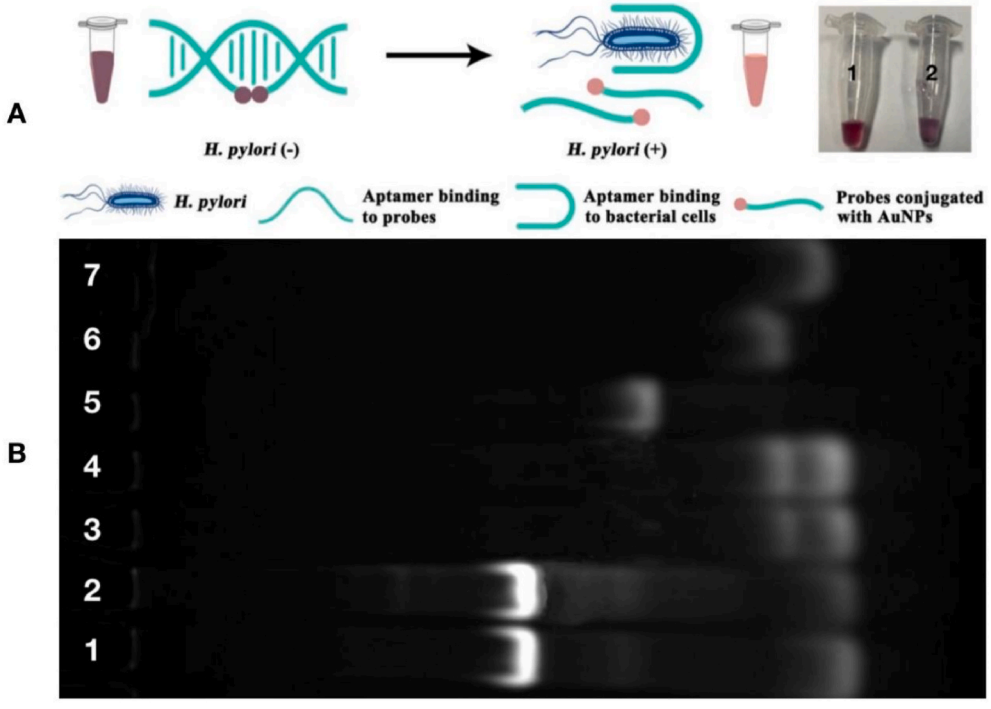

Fig. 1. The detection principle of the assay. (A) Schematic image of the colorimetric biosensing method for the detection of *H. pylori*. Inset: Tube 1: in the presence of *H. pylori* (dark red). Tube 2: in the absence of *H. pylori* (purple). (B) Gel electrophoresis image for the detection reaction. Lane 1–2: probe-1, probe-2, and aptamers; lane 3–4: probe-1, probe-2, aptamers, and *H. pylori*; lane 5: probe-2 only; lane 6: probe-1 only; lane 7: aptamers only. (For interpretation of the references to color in this figure legend, the reader is referred to the Web version of this article.)

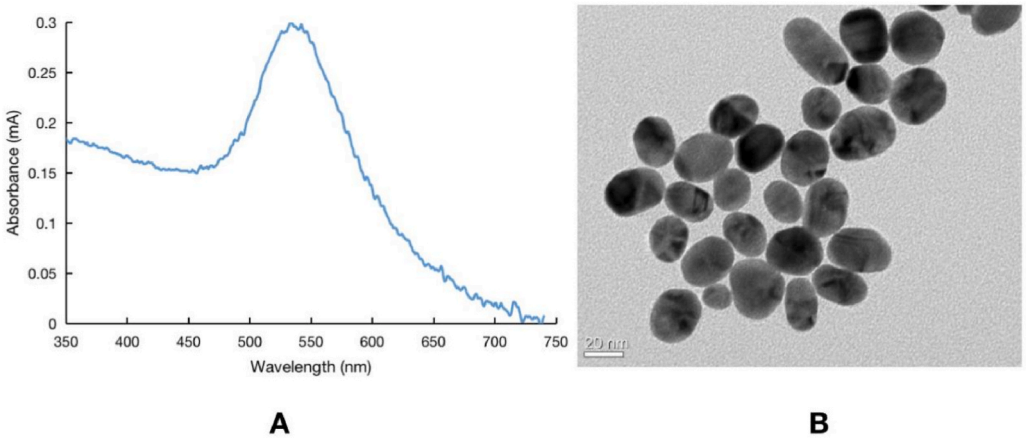

Fig. 2. Characterization of AuNPs. (A) The absorption peak of AuNP solution. (B) The surface morphology and size of AuNPs.

Table 1
Optimization of oligonucleotide probes.

Probe-1 derivatives	Sequence (5′-3′)	Probe-2 derivatives	Sequence (5′-3′)
Probe-1_{16}	SH-AATAGGGTCCTCCTGG	Probe-2_{16}	CACTGGATCTCGTCGA-SH
Probe-1_{17}	SH-GAATAGGGTCCTCCTGG	Probe-2_{17}	CACTGGATCTCGTCGAT-SH
Probe-1_{18}	SH-AGAATAGGGTCCTCCTGG	Probe-2_{18}	CACTGGATCTCGTCGATA-SH
Probe-1_{19}	SH-GAGAATAGGGTCCTCCTGG	Probe-2_{19}	CACTGGATCTCGTCGATAC-SH
Probe-1_{20}	SH-CGAGAATAGGGTCCTCCTGG	Probe-2_{20}	CACTGGATCTCGTCGATACA-SH

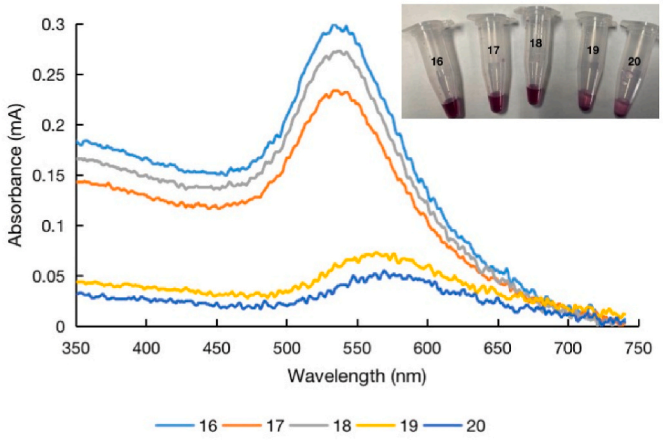

Fig. 3. Absorbance of probe pairs with different base lengths. Inset: The color comparison of five pairs of probes with different base lengths. Tube 16 represents the probe pair of Probe-1_{16} and Probe-2_{16}. Tube 17 represents the probe pair of Probe-1_{17} and Probe-2_{17}. Tube 18 represents the probe pair of Probe-1_{18} and Probe-2_{18}. Tube 19 represents the probe pair of Probe-1_{19} and Probe-2_{19}. Tube 20 represents the probe pair of Probe-1_{20} and Probe-2_{20}. (For interpretation of the references to color in this figure legend, the reader is referred to the Web version of this article.)

red. A good linear relationship with a correlation coefficient of R^2 = 0.9796 between A530 and the concentration of *H. pylori* was observed in the range of 100–1000 CFU/mL (Fig. 4B). The limit of detection (LOD) was determined by a signal-to-noise (S/N) ratio of 3:1, corresponding to 25 CFU/mL, which is better than or comparable to other reported assays (Table 2).

2.5. The specificity and reproducibility of the colorimetric biosensing method

The specificity of the colorimetric biosensing method was evaluated by performing the assay on several other bacteria, including *E. coli*, *S. aureus*, *P. aeruginosa*, *L. monocytogenes* and *S. typhimurium*. As shown in Fig. 5, the absorption peak wavelength differences between the non-*H. pylori* bacteria and blank control were small, and significant absorption peak wavelength difference was observed between the blank control and target bacteria, demonstrating the good specificity of the colorimetric biosensing method. Three such experiments were repeated, and the results showed that the fluctuation range of the absorbance value was minuscule and the standard deviation was small, indicating good reproducibility of the colorimetric biosensing assay.

2.6. Application of the colorimetric biosensing method in clinical samples

Although an indicator-based colorimetric biosensing assay has been develop to screen *H. pylori* in gastric fluids [21], whether such method could be used in stool samples is unknown. To investigate the feasibility of our method for application in clinical settings, a standard addition experiment in fecal samples was implemented. As shown in Table 3, the recoveries range from 92.0% to 114.6% and the corresponding relative standard deviations (RSDs) range from 1.75% to 13.4% for *H. pylori,* indicating that the matrix in the feces did not affect the outcome of the assay.

In addition, a total of 102 stool samples, including 35 positive samples and 67 negative samples, were examined by the colorimetric biosensing method. As expected, all samples that tested positive by C13-UBT assay were also recognized by the colorimetric biosensing method, indicating the excellent applicability of this assay in clinical samples.

3. Conclusion

In this study, we developed a novel *colorimetric biosensing method* for the rapid detection of *H. pylori* in feces. Based on the color change resulting from the aggregation or deaggregation of AuNPs, the assay can recognize even a tiny amount of *H. pylori* (25 CFU/mL) and shows high selectivity among other bacteria. Compared with C13-UBT assay, the method not only has an excellent detection speed and a lower cost, but also required no limitations to the test subjects. All these features render

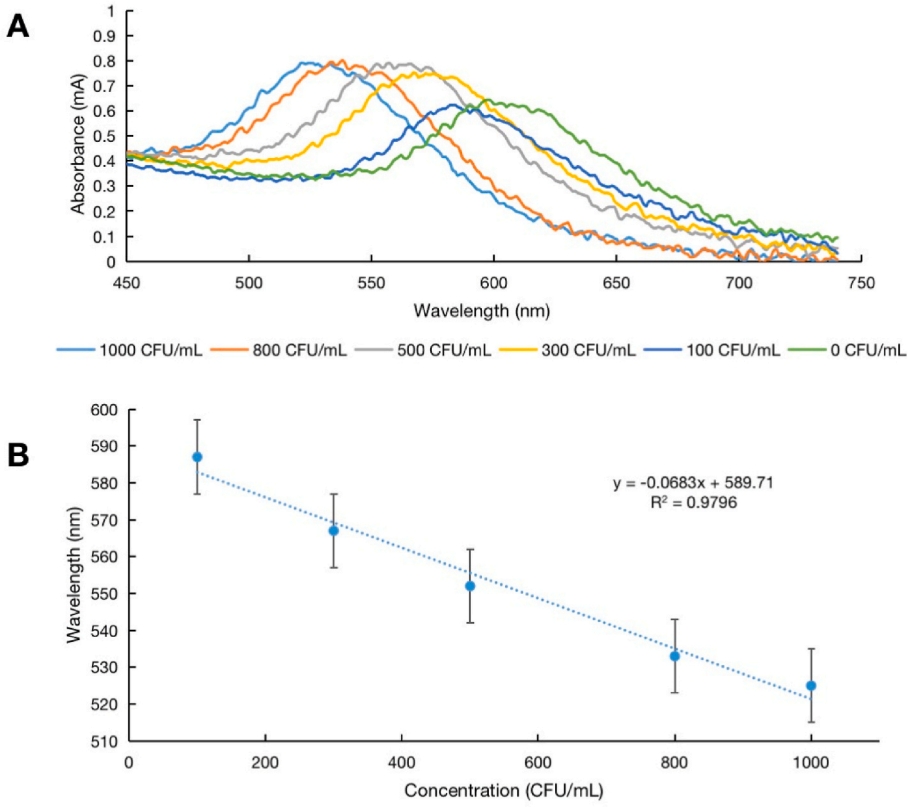

Fig. 4. The sensitivity and linear range of the colorimetric biosensing method. (A) Absorbance spectra of AuNPs in the presence of *H. pylori* at various concentrations. (B) The wavelength of the absorption peak when using different concentrations of *H. pylori*. The error bars in the figure represent the standard errors.

Table 2
The colorimetric biosensing method vs. other reported methods for *H. pylori* detection.

Title of literature	Linear Range	LOD	Reference
The development of a colorimetric biosensing assay for the rapid detection of *Helicobacter pylori* in feces	10^2–10^3 CFU/mL	25 CFU/mL	This work
Rapid detection of *Helicobacter pylori* by the naked eye using DNA aptamers	–	88 CFU/mL	[25]
The preparation of bifunctional hybrid nanoflowers and their application in the enzyme-linked immunosorbent assay for *Helicobacter pylori* detection	0–10^5 CFU/mL	50 CFU/mL	[26]
Ultrasensitive detection of *H. pylori* in human feces based on immunomagnetic bead capture and fluorescent quantum dots	10–10^6 CFU/mL	100 CFU/mL	[27]
Aptamer-superparamagnetic nanoparticles capture coupling siderophore-Fe3+ scavenging actuated with carbon dots to confer an "off-on" mechanism for the ultrasensitive detection of *Helicobacter pylori*	10–10^7 CFU/mL	1 CFU/mL	[28]
A DNAzyme-based colorimetric paper sensor for *Helicobacter pylori*	–	10^4 CFU/mL	[29]

the colorimetric biosensing assay a promising method for the clinical field detection of *H. pylori*.

4. Experimental section

4.1. Materials

The sequences of the aptamer and oligonucleotide probes used in this study are listed in Table 4. Gold(III) chloride trihydrate ($HAuCl_4$) was purchased from Sigma–Aldrich (St. Louis, MO, USA). Trisodium citrate dihydrate ($Na_3C_6H_5O_7{\cdot}2H_2O$) was purchased from Zhiyuan Chemical Reagent Co., Ltd. (Tianjin, China). Tri-(2-formylethyl) phosphine hydrochloride (TCEP) and tri-(hydroxymethyl) aminomethane (Tris) were purchased from Sangon Biotech Co., Ltd. (Shanghai, China). Unless otherwise stated, all chemicals used were of analytical grade or higher.

Bacterial strains including *Helicobacter pylori* (*H. pylori)* (ATCC 43504), *Escherichia coli* (*E. coli*) (ATCC 8099), *Staphylococcus aureus* (*S. aureus*) (ATCC 6538), *Listeria monocytogenes* (*L. monocytogenes*) (ATCC 19118) and *Pseudomonas aeruginosa* (*P. aeruginosa*) (ATCC 27853) were purchased from American Type Culture Collection (Manassas, VA, USA). *Salmonella typhimurium* (*S. typhimurium*) strain LT2 was a kind gift from Prof. Kelly Hughes at the University of Utah.

After obtaining approval from the Ethics Committee of West China Fourth Hospital of Sichuan University (ID: HXSY-EC-2021025), a total of 102 stool samples, including 35 positive and 67 negative stool samples, were collected from April 7th, 2021, to December 31st, 2021, with the criteria of "Delta Over Baseline (DOB) $\geq$ 4, positive; DOB <4, negative" by C13-UBT. Of the 102 volunteers who provided stool samples, 45 were men and 57 were women. The mean DOB of positive subjects was 23.3 and that of negative subjects was 1.6. All samples were stored at −80 °C until use.

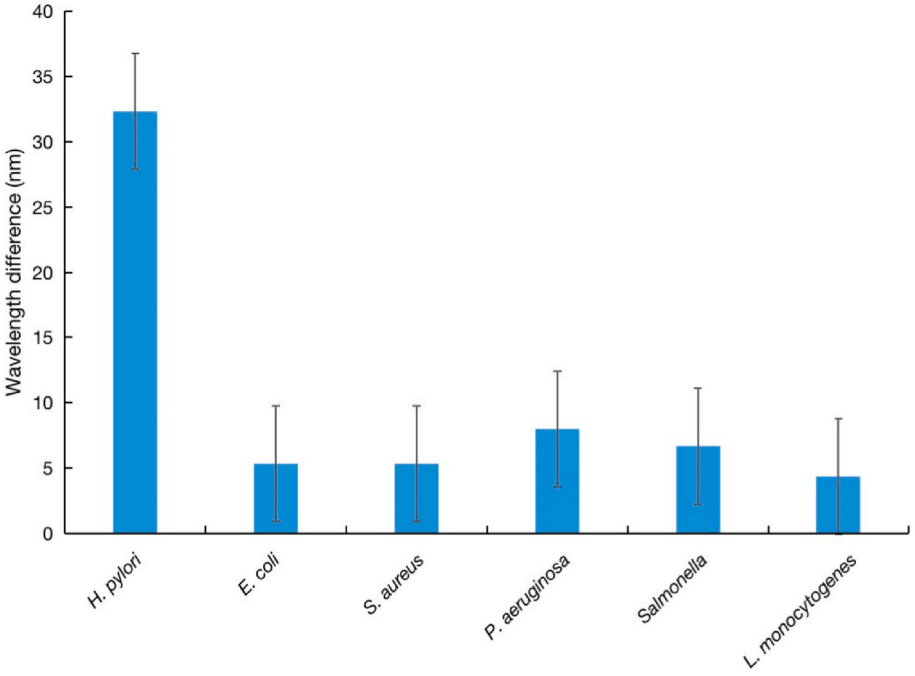

Fig. 5. The absorption peak wavelength difference between blank control and specific bacteria. The error bars in the figure represent the standard error.

Table 3
The recoveries and RSDs of this method (n = 3).

Samples	Background (CFU/mL)	Spiked (CFU/mL)	Founded (CFU/mL)	Recoveries (%)	RSDs (%)
1	520	100	590	95.2	6.11
		150	700	104.5	4.51
		200	696	96.7	1.75
2	340	100	460	104.5	10.4
		150	480	98.0	7.32
		200	575	106.5	1.89
3	140	100	275	114.6	11.1
		150	310	106.9	9.91
		200	320	94.1	5.42
4	0	100	92	92.0	13.4
		150	170	113.3	13.1
		200	211	105.5	11.3

4.2. Preparation of AuNPs

The AuNPs used in this study were prepared by the sodium citrate reduction method [30]. In brief, 15 mg of $HAuCl_4$ was dissolved in 51.5 mL of deionized water and heated to 100 °C under stirring. Then, 3.5 mL of 1% citrate solution (w/v) was added and heated until the color of the solution changed from light yellow to dark red. The AuNP solution was stored at 4 °C until use.

4.3. Functionalization of AuNPs

Twenty microliters of oligonucleotide probe (100 mM) was incubated with an equal volume of TCEP (400 mM) at room temperature for 2 h. Then, 150 μL of AuNP (50 mM) solution was added and incubated at room temperature for 4 h. Following centrifugation at 12,000 rpm at 4 °C for 30 min, the precipitate was resuspended in 200 μL of selection buffer (100 mM NaCl, 5 mM KCl, 50 mM Tris-HCl, 1 mM $MgCl_2$, pH 7.5) and stored at 4 °C until use.

4.4. The colorimetric biosensing method

The fresh colonies of each test strain were washed from the corresponding agar plates using selection buffer and adjusted to an OD600 of ~0.6. Then, 5 μL of aptamer (100 mM) was incubated with 200 μL of functionalized AuNP solution (10 mM) at room temperature for 10 min, followed by the addition of 10 μL of bacterial suspension at temperature for 10 min. The results were determined by the naked eye or by a UV-2700i spectrophotometer (Shimadzu, Japan).

4.5. Application of the colorimetric biosensing method in stool samples

A 5 × 5 mm stool sample was homogenized with 500 μL of saline. Then, 5 μL of aptamer (100 mM) was incubated with 200 μL of functionalized AuNP (10 mM) solution at room temperature for 10 min, followed by the addition of 10 μL of stool homogenate at room temperature for 10 min. The results were determined by color change with the naked eye or by UV–Vis spectrophotometry.

Subject category

DNA Recombinant techniques and nucleic acids.

Table 4
The sequences of the aptamer and probes used in this study.

Name	Sequence (5′to 3′)	Reference
Aptamer	CCAGGAGGACCCTATTCTCGTGTATCGACGAGATCCAGTG	[25]
Probe-1	SH-CGAGAATAGGGTCCTCCTGG	This study
Probe-2	CACTGGATCTCGTCGATACA-SH	This study

Funding

This study was supported by the key research and development program of Sichuan Science and Technology Department (No. 2021YFS0179).

Statement

Informed consent was obtained for this experiment.

Authors contributions

Yu Fei: Data curation, Formal analysis, Writing-Original draft, Rong Fang: Funding acquisition, Investigation, Writing-Original draft, Lina Xiao: Resources, Software, Yuqing Zhang: Validation, Ke Fan: Visualization, Yundi Jiang: Resources, Silu Lei: Visualization, Rui Xv: Resources, Dailan Yang: Software, Yan Ye: Resources, Shibing Xiang: Supervision, Ping Wang: Supervision, Chen Zhou: Conceptualization, Writing-Reviewing and Editing, Tian Tang: Methodology, Project administration, Writing-Reviewing and Editing.

Declaration of competing interest

None.

References

[1] W. Fischbach, P. Malfertheiner, Helicobacter pylori infection, Dtsch. Arztebl. Int. 115 (25) (2018) 429–436, https://doi.org/10.3238/arztebl.2018.0429.
[2] M. Leja, I. Grinberga-Derica, C. Bilgilier, C. Steininger, Review: epidemiology of Helicobacter pylori infection, Helicobacter 24 (Suppl 1) (2019), e12635, https://doi.org/10.1111/hel.12635.
[3] M. Li, Y. Sun, J. Yang, et al., Time trends and other sources of variation in Helicobacter pylori infection in mainland China: a systematic review and meta-analysis, Helicobacter 25 (5) (2020), e12729, https://doi.org/10.1111/hel.12729.
[4] Y.K. Wang, F.C. Kuo, C.J. Liu, et al., Diagnosis of Helicobacter pylori infection: current options and developments, World J. Gastroenterol. 21 (40) (2015) 11221–11235, https://doi.org/10.3748/wjg.v21.i40.11221.
[5] C.W. Huh, B.W. Kim, Diagnosis of Helicobacter pylori infection, Korean J. Gastroenterol. 72 (5) (2018 Nov 25) 229–236, https://doi.org/10.4166/kjg.2018.72.5.229. Korean.
[6] L. Demirtürk, Y. Yazgan, O. Tarçin, et al., Does N-acetyl cystein affect the sensitivity and specificity of Helicobacter pylori stool antigen test? Helicobacter 8 (2) (2003) 120–123, https://doi.org/10.1046/j.1523-5378.2003.00132.x.
[7] E.M. Inelmen, G. Gasparini, G. Sergi, G. Enzi, Evaluation of Helicobacter pylori with a stool antigen assay in frail, elderly patients, Scand. J. Gastroenterol. 40 (7) (2005) 794–799, https://doi.org/10.1080/00365520510015638.
[8] T. Shimoyama, Stool antigen tests for the management of Helicobacter pylori infection, World J. Gastroenterol. 19 (45) (2013) 8188–8191, https://doi.org/10.3748/wjg.v19.i45.8188.
[9] P. Malfertheiner, F. Megraud, C.A. O'Morain, et al., Management of Helicobacter pylori infection–the maastricht IV/florence consensus report, Gut 61 (5) (2012) 646–664, https://doi.org/10.1136/gutjnl-2012-302084.
[10] M. Nocon, A. Kuhlmann, A. Leodolter, et al., Efficacy and cost-effectiveness of the 13C-urea breath test as the primary diagnostic investigation for the detection of Helicobacter pylori infection compared to invasive and non-invasive diagnostic tests, GMS Health Technol. Assess. 5 (2009), https://doi.org/10.3205/hta000076. Doc14. Published 2009 Oct 21.
[11] C. Stoicov, R. Saffari, J. Houghton, Green tea inhibits Helicobacter growth in vivo and in vitro, Int. J. Antimicrob. Agents 33 (5) (2009) 473–478, https://doi.org/10.1016/j.ijantimicag.2008.10.032.
[12] K.E. McColl, Clinical practice. Helicobacter pylori infection, N. Engl. J. Med. 362 (17) (2010) 1597–1604, https://doi.org/10.1056/NEJMcp1001110.
[13] Y. Zhang, Y. Chen, D. Han, I. Ocsoy, W. Tan, Aptamers selected by cell-SELEX for application in cancer studies, Bioanalysis 2 (5) (2010) 907–918, https://doi.org/10.4155/bio.10.46.
[14] M.I. Shukoor, M.O. Altman, D. Han, et al., Aptamer-nanoparticle assembly for logic-based detection, ACS Appl. Mater. Interfaces 4 (6) (2012) 3007–3011, https://doi.org/10.1021/am300374q.
[15] I. Ocsoy, S. Yusufbeyoglu, V. Yılmaz, E.S. McLamore, N. Ildız, A. Ülgen, DNA aptamer functionalized gold nanostructures for molecular recognition and photothermal inactivation of methicillin-Resistant Staphylococcus aureus, Colloids Surf. B Biointerfaces 159 (2017) 16–22.
[16] D. Turek, D. Van Simaeys, J. Johnson, I. Ocsoy, W. Tan, Molecular recognition of live methicillin-resistant staphylococcus aureus cells using DNA aptamers, World J. Transl. Med. 2 (3) (2013) 67–74, https://doi.org/10.5528/wjtm.v2.i3.67.
[17] I. Ocsoy, M.A. Ocsoy, E. Yasun, W. Tan, Nucleic acid-functionalized nanomaterials, Nano LIFE (2013), 1340004, https://doi.org/10.1142/S1793984413400047, 03.
[18] C.C. Chang, C.P. Chen, T.H. Wu, C.H. Yang, C.W. Lin, C.Y. Chen, Gold nanoparticle-based colorimetric strategies for chemical and biological sensing applications, Nanomaterials 9 (6) (2019) 861, https://doi.org/10.3390/nano9060861. Published 2019 Jun 6.
[19] W. Zhao, M.A. Brook, Y. Li, Design of gold nanoparticle-based colorimetric biosensing assays, Chembiochem 9 (15) (2008) 2363–2371, https://doi.org/10.1002/cbic.200800282.
[20] E. Mauriz, P. Dey, L.M. Lechuga, Advances in nanoplasmonic biosensors for clinical applications, Analyst 144 (24) (2019) 7105–7129, https://doi.org/10.1039/c9an00701f.
[21] C. Celik, G. Can Sezgin, U.G. Kocabas, et al., Novel anthocyanin-based colorimetric assay for the rapid, sensitive, and quantitative detection of Helicobacter pylori, Anal. Chem. 93 (15) (2021) 6246–6253, https://doi.org/10.1021/acs.analchem.1c00663.
[22] L. Wang, H. Jia, Y. Sun, et al., Evaluation of NitroSpeed-Carba NP test for rapid identification among different classes of carbapenemases in Enterobacterales and Pseudomonas aeruginosa, Int. J. Infect. Dis. 106 (2021) 415–420, https://doi.org/10.1016/j.ijid.2021.04.031.
[23] C. Celik, N. Ildiz, P. Sagiroglu, M.A. Atalay, C. Yazici, I. Ocsoy, Preparation of nature inspired indicator based agar for detection and identification of MRSA and MRSE, Talanta 219 (2020), 121292, https://doi.org/10.1016/j.talanta.2020.121292.
[24] C. Celik, N. Ildiz, M.Z. Kaya, A.B. Kilic, I. Ocsoy, Preparation of natural indicator incorporated media and its logical use as a colorimetric biosensor for rapid and sensitive detection of Methicillin-resistant Staphylococcus aureus, Anal. Chim. Acta 1128 (2020) 80–89, https://doi.org/10.1016/j.aca.2020.06.005.
[25] H. Wu, L. Gu, X. Ma, et al., Rapid detection of Helicobacter pylori by the naked eye using DNA aptamers, ACS Omega 6 (5) (2021) 3771–3779, https://doi.org/10.1021/acsomega.0c05374. Published 2021 Jan 21.
[26] T. Wang, X. Li, L. Chen, et al., The preparation of bifunctional hybrid nano-flowers and their application in the enzyme-linked immunosorbent assay for Helicobacter pylori detection, Analyst 146 (1) (2021) 338–347, https://doi.org/10.1039/d0an01533d.
[27] L. Chen, X. Li, T. Zou, et al., Ultrasensitive detection of H. pylori in human feces based on immunomagnetic bead capture and fluorescent quantum dots, Analyst 144 (13) (2019) 4086–4092, https://doi.org/10.1039/c9an00193j.
[28] Z. Wang, H. Wang, X. Cheng, et al., Aptamer-superparamagnetic nanoparticles capture coupling siderophore-Fe3+ scavenging actuated with carbon dots to confer an "off-on" mechanism for the ultrasensitive detection of Helicobacter pylori, Biosens. Bioelectron. 193 (2021), 113551, https://doi.org/10.1016/j.bios.2021.113551.
[29] M.M. Ali, M. Wolfe, K. Tram, et al., A DNAzyme-based colorimetric paper sensor for Helicobacter pylori, Angew Chem. Int. Ed. Engl. 58 (29) (2019) 9907–9911, https://doi.org/10.1002/anie.201901873.
[30] X. Ji, X. Song, J. Li, Y. Bai, W. Yang, X. Peng, Size control of gold nanocrystals in citrate reduction: the third role of citrate, J. Am. Chem. Soc. 129 (45) (2007) 13939–13948, https://doi.org/10.1021/ja074447k.